Degradation Process of Lead Chromate in Paintings by Vincent van Gogh Studied by Means of Spectromicroscopic Methods. Part 5. Effects of Nonoriginal Surface Coatings into the Natur...

ARTICLE *in* ANALYTICAL CHEMISTRY · OCTOBER 2014

Impact Factor: 5.64 · DOI: 10.1021/ac502841g · Source: PubMed

analytical chemistry

Article

pubs.acs.org/ac

Degradation Process of Lead Chromate in Paintings by Vincent van Gogh Studied by Means of Spectromicroscopic Methods. Part 5. Effects of Nonoriginal Surface Coatings into the Nature and Distribution of Chromium and Sulfur Species in Chrome Yellow Paints

Letizia Monico,*[,†,‡] Koen Janssens,[‡] Frederik Vanmeert,[‡] Marine Cotte,[§,∥] Brunetto Giovanni Brunetti,[†] Geert Van der Snickt,[‡] Margje Leeuwestein,[⊥] Johanna Salvant Plisson,[#] Michel Menu,[#,¶] and Costanza Miliani[†]

[†]Institute of Molecular Science and Technologies (ISTM), National Research Council (CNR) and Centre SMAArt, c/o Department of Chemistry, Biology and Biotechnologies, University of Perugia, via Elce di Sotto 8, 06123 Perugia, Italy

[‡]Department of Chemistry, University of Antwerp, Groenenborgerlaan 171, 2020 Antwerp, Belgium

[§]European Synchrotron Radiation Facility, Avenue des Martyrs 71, 38000 Grenoble, France

[∥]Laboratoire d'Archéologie Moléculaire et Structurale, CNRS-UPMC, UMR 8220, place Jussieu 4, 75005 Paris, France

[⊥]Kröller-Müller Museum, Houtkampweg 6, 6731 AW Otterlo, The Netherlands

[#]Centre de Recherche et de Restauration des Musées de France (C2RMF), Palais du Louvre, Quai François Mitterrand 14, 75001 Paris, France

[¶]Institut de Recherche de Chimie Paris, CNRS − Chimie ParisTech, UMR 8247, rue Pierre et Marie Curie 11, 75005 Paris, France

Supporting Information

ABSTRACT: The darkening of lead chromate yellow pigments, caused by a reduction of the chromate ions to Cr(III) compounds, is known to affect the appearance of several paintings by Vincent van Gogh. In previous papers of this series, we demonstrated that the darkening is activated by light and depends on the chemical composition and crystalline structure of the pigments. In this work, the results of Part 2 are extended and complemented with a new study aimed at deepening the knowledge of the nature and distribution of Cr and S species at the interface between the chrome yellow paint and the nonoriginal coating layer. For this purpose, three microsamples from two varnished paintings by Van Gogh and a waxed low relief by Gauguin (all originally uncoated) have been examined. Because nonoriginal coatings are often present in artwork by Van Gogh and contemporaries, the understanding of whether or not their application has influenced the morphological and/or physicochemical properties of the chrome yellow paint underneath is relevant in view of the conservation of these masterpieces. In all the samples studied, microscopic X-ray fluorescence (μ-XRF) and X-ray absorption near edge structure (μ-XANES) investigations showed that Cr(III)-based alteration products are present in the form of grains inside the coating (generally enriched of S species) and also homogeneously widespread at the paint surface. The distribution of Cr(III) species may be explained by the mechanical friction caused by the coating application by brush that picked up and redistributed the superficial Cr compounds, likely already present in the reduced state as result of the photodegradation process. The analysis of the XANES profiles allowed us to obtain new insights into the nature of the Cr(III) alteration products, that were identified as sulfate-, oxide-, organo-metal-, and chloride-based compounds. Building upon the knowledge acquired through the examination of original paint samples and from the investigation of aged model paints in the last Part 4 paper, in this study we aim to characterize a possible relation between the chemical composition of the coating and the chrome yellow degradation pathways by studying photochemically aged model samples covered with a dammar varnish contaminated with sulfide and sulfate salts. Cr speciation results did not show any evidence of the active role of the varnish and added S species on the reduction process of chrome yellows.

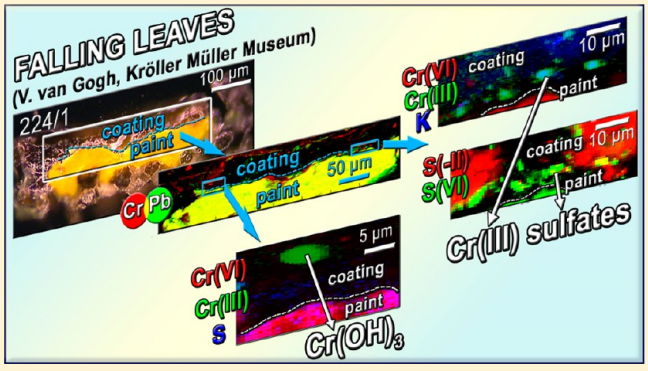

Received: July 30, 2014
Accepted: October 10, 2014
Published: October 10, 2014

The darkening of chrome yellows ($PbCr_{1-x}S_xO_4$, $0.0 \leq x \leq 0.8$) is a phenomenon that affects many paintings of the Impressionist and post-Impressionist period,[1,2] posing a challenge for both their visual appreciation and conservation care.

Synchrotron radiation (SR)-based X-ray microprobe techniques [e.g., micro X-ray absorption near edge structure (μ-XANES), micro-X-ray fluorescence (μ-XRF) spectroscopy and micro-X-ray diffraction (μ-XRD)] and scanning transmission electron microscopy (STEM) coupled to energy electron loss spectroscopy (EELS) investigations have recently provided direct evidence that the chrome yellow alteration is due to a reduction of the chromate ion.[3−5] By studying photochemically aged oil paint models containing different chrome yellow varieties, it has been found that the photoreduction is favored when the pigment is in the form of a S-rich orthorhombic $PbCr_{1-x}S_xO_4$ coprecipitate ($x > 0.4$), rather than monoclinic $PbCrO_4$.[3,4]

XRD, Raman, and Fourier transform infrared (FTIR) spectroscopy measurements on paintings and original microsamples established that light-sensitive forms of chrome yellow were widely used by Van Gogh and contemporaries, such as, for example, Cézanne and Gauguin.[6−8]

As observed with the aged paint models, SR-based X-ray analysis proved that the chromium reduction is also the cause of the darkening observed in the yellow paint microsamples taken from a selection of Van Gogh paintings. In all these cases, the presence of a nonoriginal coating was found, that was applied later, even decades after the paintings were completed.[5,9]

Earlier studies on two Van Gogh paintings[10,11] suggested that the application of a nonoriginal coating may influence the original properties of the components of the paint layer. In *Flowers in a Blue Vase* [Kröller-Müller Museum (KMM), Otterlo, NL], it has been observed that the varnish can act as an important factor in the degradation process of the cadmium yellow (CdS) paint underneath. The interactions between $CdSO_4$ (the primary photo-oxidation product of the original CdS pigment), lead-based driers, and oxalate ions contained in the nonoriginal overlying coating were suggested to lead to the formation of $PbSO_4$ and CdC_2O_4.[10]

In a selection of the orange paint areas of *Falling Leaves* (*Les Alyscamps*) (KMM), solvents that were used to apply the varnish were hypothesized as possible triggering agents in the formation of zinc carboxylate-based protrusions.[11]

The examination of the chemical composition and spatial distribution of the main constituting components of both the chrome yellow-based layer and the coating is therefore relevant in order to understand whether or not the presence of the nonoriginal overlying material in some way affects the morphological and/or physicochemical properties of the paint itself.

For this purpose, in the following sections, we present and discuss the results obtained from the study of three degraded chrome yellow paint microsamples taken from the two Van Gogh varnished paintings *Falling Leaves* (*Les Alyscamps*) (KMM) and *Bank of the Seine* [Van Gogh Museum (VGM), Amsterdam, NL] and the wax-coated low relief *Be Mysterious* (*Soyez Mystérieuses*) by Gauguin [Musée d'Orsay (M'O), Paris, FR].

SR-based Cr and S K-edge μ-XANES and μ-XRF analysis were used to study the distribution of Cr and S species at different oxidation states within the various layers of the samples, whereas knowledge on the molecular composition of coatings was acquired using infrared and Raman spectroscopy.

The results obtained were complemented with SR-based Cr K-edge X-ray investigations performed on photochemically aged $PbCrO_4$/$PbCr_{0.2}S_{0.8}O_4$ oil paint models, covered with an ad hoc prepared varnish, composed by a dammar resin contaminated with a small amount of sulfur-based salts, that are reported to act as potential reducing agents of chromate ions.[12−15]

EXPERIMENTAL SECTION

Resin-Embedded Original Paint Microsamples. Investigations were performed on three already available resin-embedded paint microsamples taken from darkened chromium-based yellow areas of the two varnished Van Gogh paintings *Falling Leaves* (*Les Alyscamps*) (sample 224/1) and *Bank of the Seine* (sample F293/3) and the waxed low relief *Be Mysterious* (*Soyez Mystérieuses*) by Gauguin (sample 2751) [Figure S-1, Supporting Information (SI); Figures 2A−4A]. The selected materials were previously investigated using SEM-EDX, FTIR and Raman spectroscopy, demonstrating the presence of the chrome yellow in the $PbCr_{1-x}S_xO_4$ form.[6] Further details about these samples are reported in Table S-1 (SI).

Preparation of Varnished Oil Paint Models and Photochemical Aging Protocol. Paint models were made by mixing either monoclinic $PbCrO_4$ or $PbCr_{0.2}S_{0.8}O_4$ with linseed oil in a 4:1 weight ratio and painting the mixtures out on polycarbonate microscope slides. In line with previous papers,[4,6,8] we will designate these two materials below as S_{1mono} and S_{3D}, respectively. Once the oil paints were dried (after about 30 days), a dammar resin (Zecchi) was dissolved in turpentine. In order to introduce sulfur species, the resin was mixed with about 1−2 wt % of either $BaSO_4$ ($S_{1mono\text{-}SO_4}{}^{2-}$, $S_{3D\text{-}SO_4}{}^{2-}$) or ZnS ($S_{1mono\text{-}S^{2-}}$, $S_{3D\text{-}S^{2-}}$) (both Sigma-Aldrich). The mixture thus obtained was applied at the surface of each sample as a layer of ca. 50 μm in thickness. Despite the fact that these models are not representative of most of the paintings both in terms of morphology and chemical composition, they are useful for the diffusion of S species into a coating.

The photochemical aging was performed by exposing paint models for 98 h to the UVA-visible/NIR light (300−1100 nm) emitted by a 175 W UV-filtered Cermax xenon lamp (mod. PE175BUV, Excelitas Technologies) and at 40% of relative humidity condition. The measured illuminance at the sample position was about $1.7 \cdot 10^5$ lux.

Methods. The following spectroscopic methods were used to investigate original samples and varnished paint models: micro-Raman, reflection mode micro-FTIR, SR-based Cr and S K-edge μ-XANES, and μ-XRF [both performed at the beamline ID21[16] of the European Synchrotron Radiation Facility (ESRF, Grenoble, FR)]. Regarding sample F293/3, because results obtained at the Cr K-edge were already presented in Part 2,[9] only S K-edge analysis will be discussed below. Details about the instruments and the experimental conditions are described in the SI.

RESULTS AND DISCUSSION

Original Paint Microsamples: Spectroscopic Characterization of the Coatings. Figure 1 shows the IR and Raman profiles collected from the darkened nonoriginal coatings (ca. 50−100 μm in thickness) of paint microsamples 224/1, 2751 and F293/3 (cf. Figures 2A−4A). Available details on past treatments of the corresponding artworks are reported in Table S-1 (SI).

Regarding 224/1 [from *Falling Leaves* (*Les Alyscamps*)], IR derivative-shape signals at around 1450 and 1380 cm^{-1} (Figure 1A; black line on top) are ascribable to a terpenic resin. This result is consistent with those reported by a previous study,[11] obtained analyzing other samples originating from different locations of

dx.doi.org/10.1021/ac502841g | *Anal. Chem.* 2014, 86, 10804−10811

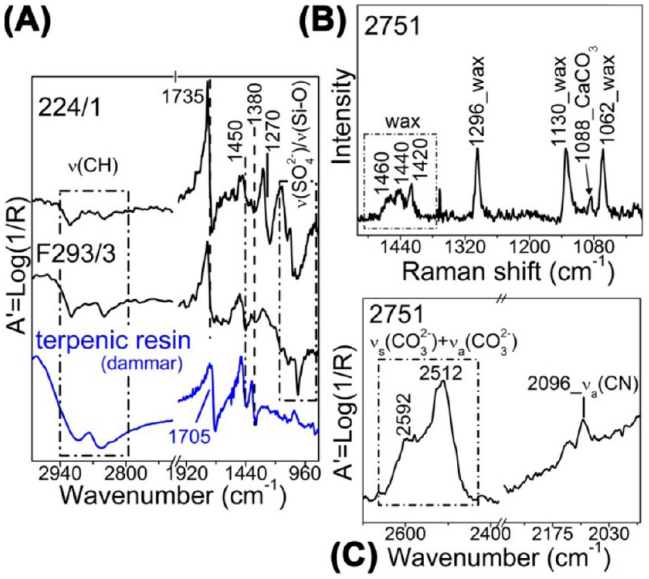

Figure 1. (A) Reflection micro-FTIR spectra collected from the varnish layer of 224/1 and F293/3 (black) compared to that of a terpenic resin (blue). (B) Raman and (C) reflection mode micro-FTIR spectra obtained from the varnish layer of 2751 (cf. Figures 2A–4A, to see the photomicrographs of these samples).

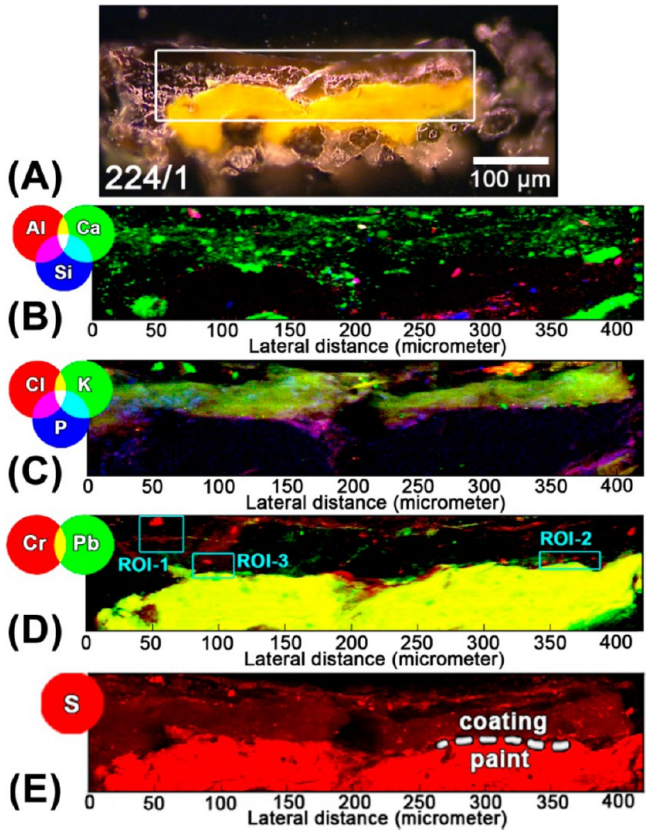

Figure 2. Sample 224/1 [*Falling Leaves* (*Les Alyscamps*)]: (A) photomicrograph and RGB composite images of (B) Al/Ca/Si, (C) Cl/K/P, (D) Cr/Pb, (E) S. The maps shown in (B–D) were obtained by μ-XRF at a primary beam energy of 6.086 keV (map size: 420 × 87 μm^2; pixel size: 1 × 0.5 μm^2; dwell time: 150 ms), whereas that illustrated in (E) at 2.520 keV (map size: 420 × 89 μm^2; pixel size: 1 × 1 μm^2; dwell time: 150 ms). Mapping experiments were performed in the region indicated by the white rectangle in (A). In (D), the cyan rectangles show the regions of interest in which more detailed μ-XRF and μ-XANES analyses were performed (cf. Figure 5). The sampling location of 224/1 is reported in Figure S-1A (SI).

the same painting. Due to the derivative-shape bands at ca. 1270 and 1735 cm^{-1} (ester C═O asymmetric stretching),[17] the latter shifted toward higher wavenumbers with respect to that of a terpenic resin (ca. 1705 cm^{-1}; Figure 1A, blue line), the additional presence of a synthetic resin cannot be excluded. In this energy range, the contribution from lipids (e.g., due to a drying oil) cannot be discarded as well, because of its IR intense signal at around 1745 cm^{-1}.[18] In the 1100–1000 cm^{-1} range, a detailed interpretation of the vibrational modes of the organic materials is made difficult due to the overlap with fundamental modes of sulfates and/or silicates (see below for a detailed discussion).

For F293/3 (from *Bank of the Seine*), IR bands at 1735, 1450, and 1380 cm^{-1} (Figure 1A, black line on middle) suggests again that a terpenic resin and lipids are the main organic constituents of the coating.

While Raman spectroscopy did not give direct insights into the chemical compositions of the varnish layer of 224/1 and F293/3 due to the high fluorescence background signal, for sample 2751 (from *Be Mysterious*), it permitted a natural wax to be confirmed as the main constituent of the surface coating (Table S-1, SI). In Figure 1B, this is demonstrated by the presence of signals at 1062, 1130, 1296, 1420, 1440, and 1460 cm^{-1}.[19]

SR-based μ-XRF mapping experiments revealed that the varnish/wax layers of all the samples are locally rich in Al and Si-based grains (Figures 2B–4B and Figure 4 of Part 2[9]), suggesting the presence of aluminum silicate-based compounds. Micro-FTIR spectroscopy points to the presence of this class of material by the fundamental Si–O stretching mode at 1100–1010 cm^{-1} (Figure 1A); two characteristic sharp signals at 3698 and 3620 cm^{-1} (not shown in Figure 1) are ascribable to the OH stretching modes of kaolin [$(AlSi_3,Si_4)O_{10}(OH)_2$].[20] Because the coatings resulted enriched in S and other elements, such as Ca, Ba, and K (Figures 2B,C,E, 3B–D, 4B,C), and considering that the IR fundamental SO_4^{2-} stretching mode may overlap with that of silicate,[20] also the presence of sulfate-based compounds (e.g., $CaSO_4$, $BaSO_4$, K_2SO_4) cannot be excluded.

In the Ca-rich areas of 2751 (Figure 3C), $CaCO_3$ was identified by its Raman signal at 1088 cm^{-1} and the IR combination band from the CO_3^{2-} stretching and bending at about 2592 and 2512 cm^{-1} (Figure 1B,C).[19,20] A cyano-based compound was also revealed by IR spectroscopy (C≡N asymmetric stretching, 2096 cm^{-1}) (Figure 1C).[21]

The diffuse presence of Cl and P was detected in the varnish layer of 224/1 (Figure 2C), while in case of F293/3 only Cl was revealed (Figure 4 of Part 2[9]).

The source of provenience of the above-mentioned materials is not yet clear: they can be due either to impurities of the nonoriginal coating, or other conservation materials applied in the past (e.g., glue used for the facing/lining), or atmospheric pollutants (gases, airborne particles) deposited on the surface.[22–26]

Inside the coatings of all samples, Cr-rich particles (Figures 2D–3D, 4B), which most likely originally belonged to the lead chromate-based paint below, are also present, often associated with S species. The latter are diffused within the coating as well (Figures 2E, 3D, 4C).

Because several studies report that S species (e.g., sulfides) can locally act as redox partner for the Cr(VI) reduction,[12–15] the next section will focus on the discussion of the Cr and

dx.doi.org/10.1021/ac502841g | *Anal. Chem.* 2014, 86, 10804–10811

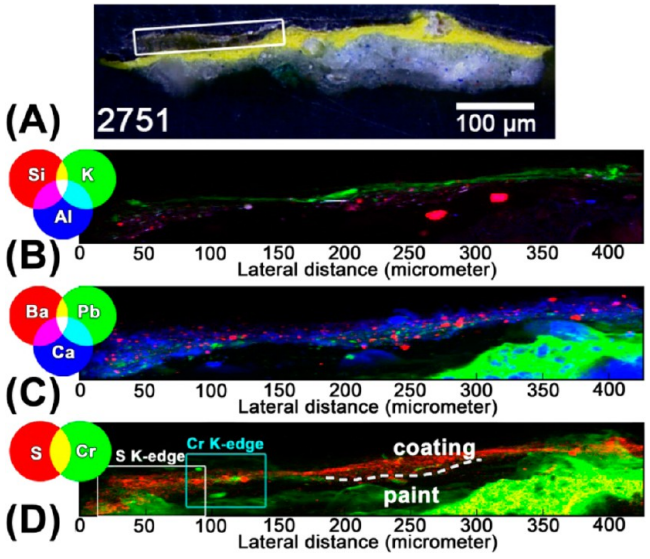

Figure 3. Sample 2751 (*Be Mysterious*): (A) photomicrograph and RGB composite images of (B) Si/K/Al, (C) Ba/Pb/Ca and (D) S/Cr (map size: 426 × 70 μm^2; pixel size: 1 × 0.5 μm^2; dwell time: 150 ms). Maps were acquired from the region illustrated by the white rectangle in (A). In (D), the cyan and white rectangles indicate the region of interest in which detailed Cr and S K-edge μ-XRF and μ-XANES investigations were performed (cf. Figure 6). The sampling area of 2751 is reported in Figure S-1B (SI).

S-speciation results obtained from the investigations of selected areas localized inside the surface coating and/or at the interface with the yellow paint of the above-mentioned samples.

Original Paint Microsamples: Cr- and S-Speciation Measurements and Chemical State Mapping. Cr and S K-edge μ-XANES and μ-XRF were performed in the regions of interest shown in Figures 2D−3D and 4A, and the corresponding results are presented in Figures 4−6, respectively. The relative abundance of Cr and S species (expressed as [Cr(III)]/[Cr_{total}] and [S(VI)]/[S_{total}]) were obtained by linear combination fitting of the XANES spectra (Figures 4D, 5D,E, 6C,D) and are summarized in Table S-2 (SI).

Sample 224/1 [Falling Leaves (Les Alyscamps)]. The chemical state maps of Cr and S (Figure 5A_1−C) exhibit distinct distributions. Sulfates [S(VI)] and chromates [Cr(VI)] are localized within the yellow paint (ROI-2 and 3), whereas sulfur in the varnish layer is mainly present as sulfides [S(-II)], with the exception of a few sulfate grains (ROI-1 and 2). Cr(III)-rich particles, often associated with the presence of sulfates (ROI-1 and 2), are localized nearby the interface with the yellow paint (ROI-2 and 3) and diffused inside the varnish (ROI-1). In the latter location, reduced and unreduced Cr species are homogeneously widespread nearby the Cr(III)-rich grain.

XANES measurements confirm that Cr(III) and S(VI) species are the main constituents of the grains embedded in the varnish, as suggested by a low intense pre-edge peak at 5.993 keV[3,27] and the intense white line at around 2.482 keV[28,29] in the Cr and S K-edge XANES spectra, respectively (Figure 5D,E, $FL01_{Cr/S}$-$FL04_{Cr/S}$; due to the similar spectral features only a selection of these data is shown). In the S K-edge XANES profiles, a weak signal at around 2.473 keV suggests S(-II) species to be present as well [ca. 10−20%; see Table S-2 (SI) for details about the fitting results]. Spectra are well described by including Cr(III) sulfate-based compounds [$Cr_2(SO_4)_3{\cdot}H_2O$ and/or $KCr(SO_4)_2{\cdot}12H_2O$] as components of the fitting model (Figure S-2 of SI to see an

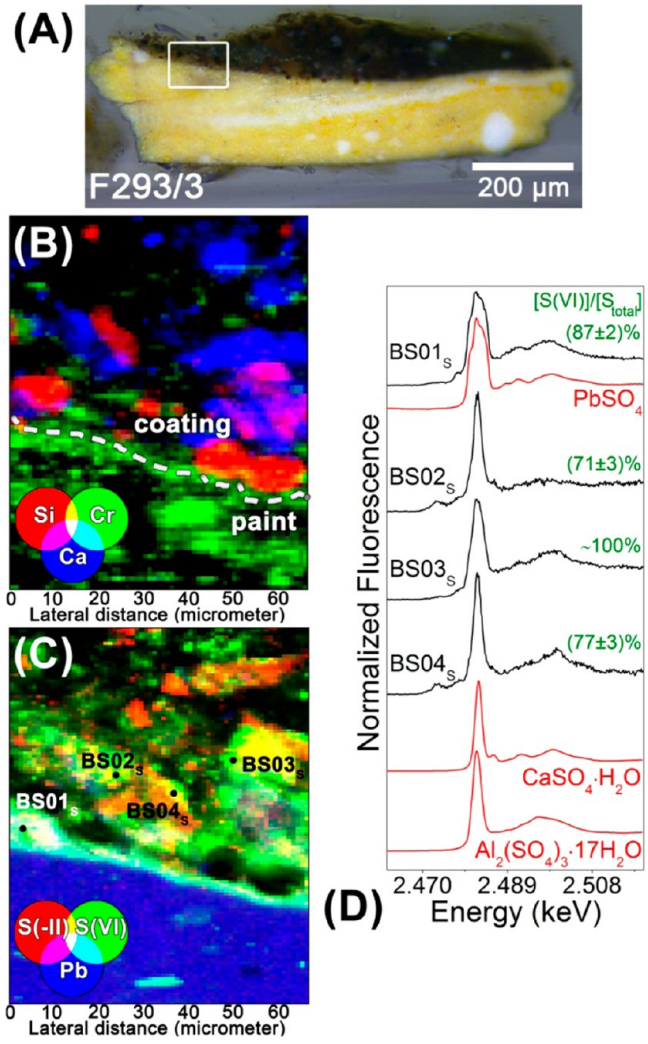

Figure 4. Sample F293/3 (*Bank of the Seine*): (A) photomicrograph and RGB composite images of (B) Si/Cr/Ca (dwell time: 300 ms; pixel size: 1 × 1 μm^2; primary beam energy: 6.086 keV) and (C) S(-II)/S(VI)/Pb (dwell time: 150 ms; pixel size: 1 × 0.7 μm^2; primary beam energy: 2.473−2.520 keV). Maps were acquired in the area shown by the white rectangle in (A). (D) S K-edge XANES spectra collected from the areas indicated in (C). In red, spectra of the reference compounds. Green labels report the percentage relative amount of S(VI) [Table S-2 (SI)]. The sampling area of F293/3 is shown in Figure S-1C (SI).

example). Moreover, in the S K-edge XANES profile, good results in the energy spectral range of reduced S species are obtained including the KSCN profile in the fit (Table S-2, SI). Although no evidence of the presence of a cyano-based compound was obtained using FTIR, we consider the presence of this material to be plausible, because it is reported as an agent employed to improve the resistance and hardness of the synthetic resin constituting the varnish.[30,31]

In another region of the coating (Figure 5D,E, $FL05_{Cr/S}$), Cr(III) species are present in a relative abundance around 70%, whereas that of S(-II) species increases, reaching an amount of ca. 35% (Table S-2, SI). In a S-free area (Figure 5D, $FL07_{Cr}$), the Cr appears to be completely reduced to the Cr(III) state as well, the corresponding XANES spectrum resembling that of $Cr(OH)_3$.

Because in this and another of the samples examined (see next paragraph) these particles are encountered only at the

dx.doi.org/10.1021/ac502841g | *Anal. Chem.* 2014, 86, 10804−10811

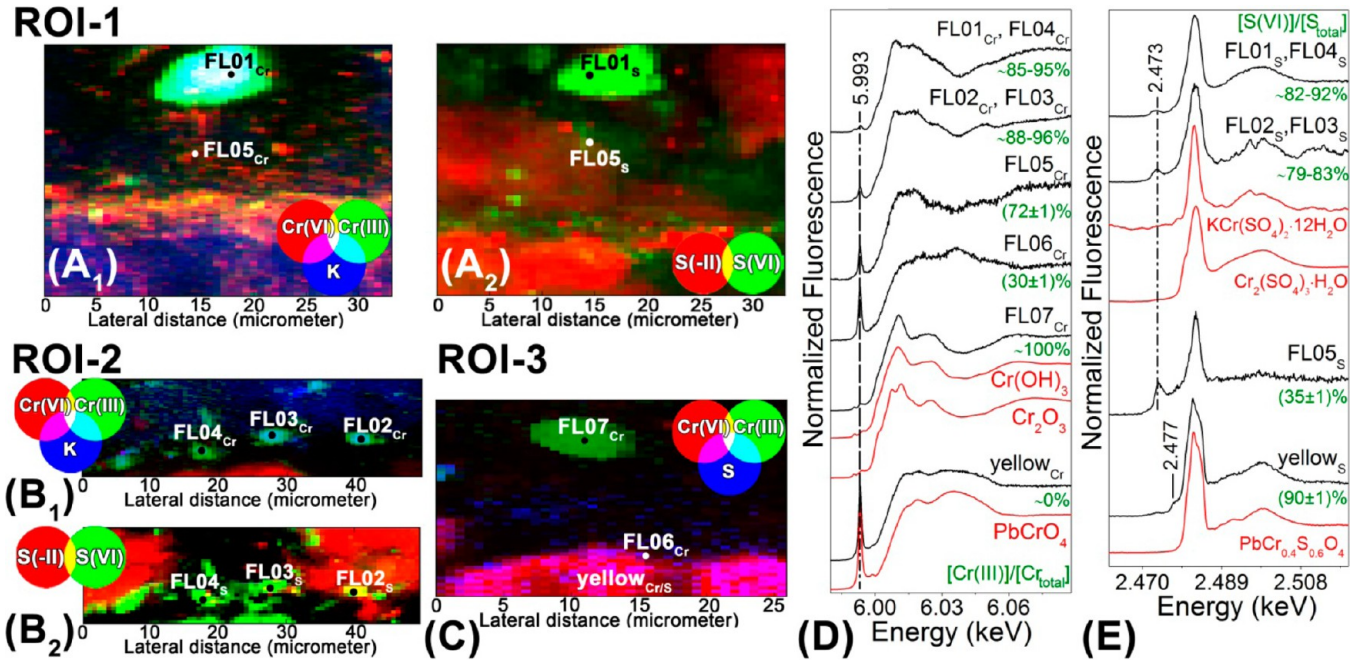

Figure 5. Sample 224/1 [*Falling Leaves (Les Alyscamps)*]: RGB chemical state maps of (A_1,B_1, C) Cr(VI)/Cr(III) and (A_2,B_2) S(-II)/S(VI). In blue, distribution of (A_1,B_1) K and (C) S (dwell time: 150 ms; pixel size Cr K-edge: 0.7 × 0.25 μm^2; pixel size S K-edge: 0.7 × 0.5 μm^2). The mapping experiments locations are shown in Figure 2D. (D) Cr and (E) S K-edge XANES spectra. Analysis positions are indicated in (A–C). In red, profiles of the reference compounds. Green labels indicate the percentage relative amount of S(VI) and Cr(III) [Table S-2 (SI)].

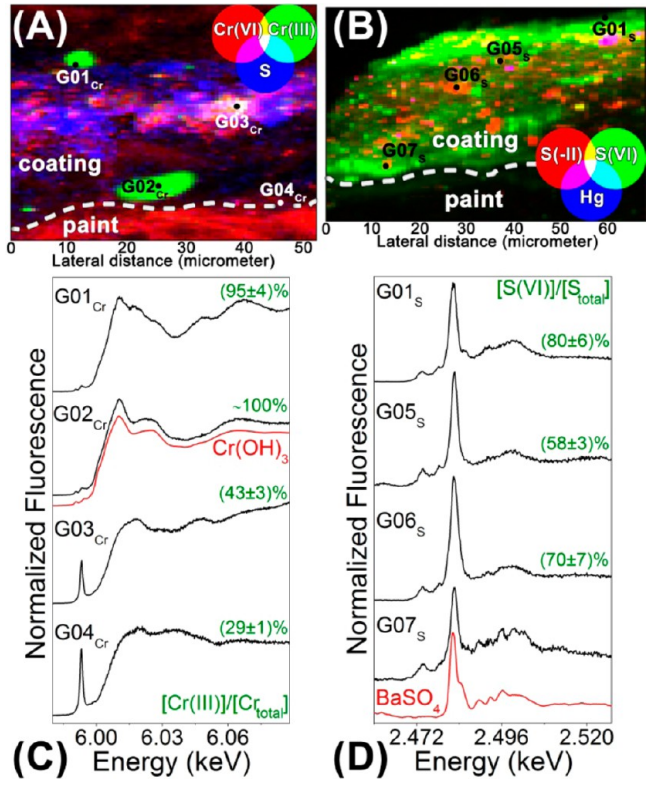

Figure 6. Sample 2751 (*Be Mysterious*): RGB μ-XRF chemical state maps of (A) Cr(VI)/Cr(III)/S_{total} and (B) S(-II)/S(VI)/Hg (dwell time: 150 ms; pixel size Cr K-edge: 0.7 × 0.5 μm^2; pixel size S K-edge: 1 × 0.5 μm^2). The mapping experiments locations are shown in Figure 3D. (C) Cr and (D) S K-edge XANES spectra. Measurement positions are indicated in (A,B). In red, spectra of the reference compounds. Green labels indicate the percentage relative amount of S(VI) and Cr(III) [Table S-2, (SI)].

paint/varnish interface, we do not think that they were originally present [e.g., as viridian (Cr_2O_3·$2H_2O$), a pigment often used by Van Gogh and contemporaries],[1,2] but rather, they are the products of the degradation process.

A fairly low relative amount of Cr(III) (around 30%) was encountered at the yellow paint/varnish interface (Figure 5D, $FL06_{Cr}$), whereas no Cr(III) species were found inside the yellow paint underneath. In the latter area, the Cr and S K-edge XANES spectra are more similar to that of either $PbCrO_4$ or $PbCr_{0.4}S_{0.6}O_4$ references (Figure 5D,E, $yellow_{Cr/S}$). In the S K-edge XANES profile, the presence of an additional weak signal at 2.477 keV is ascribable to sulfite species (ca. 10 wt %).[28,29]

Sample 2751 (Be Mysterious). Similar to 224/1, the Cr chemical state maps acquired from 2751 (Figure 6A) reveal that Cr (III)-based compounds are present as grains inside the wax layer and nearby the yellow paint surface. S(VI) species [sometimes associated with Cr(III) species] are spread inside the coating (Figure 6B), although sulfides are present in the form of "islands". The latter are sometimes colocalized with Hg, suggesting the presence of vermilion (HgS), a pigment often used by artists of this period[1,2] and likely present as an impurity.

In two positions, Cr K-edge XANES spectra reveal that Cr is as about 100% in Cr(III)-state (Figure 6C, $G01_{Cr}$-$G02_{Cr}$). Notably, in a S-free area, the profile resembles that of the $Cr(OH)_3$ reference ($G02_{Cr}$). In a sulfate-rich location, the spectrum ($G01_{Cr}$) is well described by a combination of the XANES profiles of $Cr(OH)_3$ and $KCr(SO_4)_2$·$12H_2O$. Due to the similarities among the spectra of different Cr(III)-sulfate based compounds [e.g., $(NH_4)_2SO_4Cr_2(SO_4)_3$·$24H_2O$, $KCr(SO_4)_2$·$12H_2O$ and $Cr_2(SO_4)_3$·H_2O], all fitting models yield approximately the same $Cr(III)/Cr_{total}$ ratio (Table S-2, SI).

The S K-edge XANES analysis performed in the same area (Figure 6D, $G01_S$) reveals the presence of a mixture of S(VI)- and S(-II) species in a relative amount of ca. 80% and 20%, respectively (Table S-2, SI). Here, the sulfate is likely present as a

dx.doi.org/10.1021/ac502841g | *Anal. Chem.* 2014, 86, 10804–10811

mixture of $(NH_4)_2SO_4Cr_2(SO_4)_3{\cdot}24H_2O$ and gypsum ($Ca_2SO_4{\cdot}2H_2O$), whereas reduced sulfur could be present as a SCN-based compound. The latter observation is supported by the FTIR data of Figure 1C.

In another S-rich area inside the wax layer (Figure 6D, $G03_{Cr}$), the Cr K-edge XANES allowed a relative amount of Cr(VI) of around 45% to be estimated (S K-edge profile not available).

The S K-edge XANES spectra obtained from two other Ca, Al, and Si-rich regions of the coating (Figure 6E, $G05_S$-06_S; Cr K-edge spectrum not available) are well described by including the profiles of $Ca_2SO_4{\cdot}2H_2O$, Ca−K based aluminum silicate sulfate compounds and KSCN in the fit. In these areas, the relative amount of S(VI) is about 60−70% (Table S-2, SI).

In a Ba-rich location (Figure 6D, $G07_S$), despite the fact that the fitting procedure did not yield good results, the spectrum resembles that of $BaSO_4$. The presence of a weak peak at 2.473 keV suggests also the presence of smaller amount of reduced sulfur. At the yellow paint/coating interface, the fitting of the Cr K-edge XANES profile (Figure 6C, $G04_{Cr}$; S K-edge spectrum not available) yields a relative abundance of Cr(III) of about 30% (Table S-2, SI).

Sample F293/3 (Bank of the Seine). Similar to the cases discussed above, previous Cr speciation investigations of F293/3 (Figure 6 of Part 2[9] to see the corresponding XANES profiles) revealed that Cr(III) compounds are present in the form of grains inside the varnish layer, reaching a relative amount of around 90% (Table S-2 of SI, 03 and 07). Reduced Cr is also widespread both in the areas nearby these grains and those the paint surface in a relative amount between 15 and 50% (Table S-2 of SI, 01−02 and 04−06).

S K-edge μ-XRF maps (Figure 4C) show that S(VI) species are widespread within the varnish, while S(-II) species are localized in some areas. At the white-yellow paint/coating interface, the close spatial correlation between sulfate and Pb suggests the presence of $PbSO_4$.

The above-mentioned observations could be confirmed by S K-edge XANES point measurements (not acquired in the same areas of the Cr K-edge XANES spectra described in Part 2[9]): the profiles obtained from the Pb-rich locations resemble to that of the $PbSO_4$ reference (Figure 4D, $BS01_s$ and $BS03_s$), although in other regions, gypsum mixed with either aluminum sulfate ($BS02_s$) or $PbSO_4$ ($BS04_s$) was detected. In the latter two areas, the relative abundance of reduced sulfur was estimated to be around 20−30% (Table S-2, SI).

In summary, we can conclude that the three original samples here investigated are characterized by the presence of reduced Cr compounds that are localized as grains inside the S-rich areas of the varnish/wax layer and at the yellow paint/coating interface. On the basis of the knowledge previously acquired on paint models,[4] we consider it very probable that Cr(III) species, identified as sulfate-, oxide-, organo-metal- and chloride-based compounds, are products of the degradation process of the original $PbCr_{1-x}S_xO_4$ (with $x \sim 0.1$ for F293/3, $x \sim 0.5$ for 224/1 and 2751; Table S-1 of SI).

Upon light exposure, whether or not the chromates have reacted with the organic matter of the varnish, with the sulfur species contained in it, or with both of them is not clear, although the model discussed in a previous study assumes that both could have a significant role in the reduction.[5] Other studies on artificially aged zinc yellow ($K_2O{\cdot}4ZnCrO_4{\cdot}3H_2O$) oil paint models revealed that atmospheric gaseous pollutant SO_2, in combination with different relative humidity conditions, favors the degradation of the original pigment, leading to the formation of secondary Cr(III) and dichromate species.[32]

A first attempt aimed at obtaining a better view of the possible active role of the coating and some of its additional components (e.g., S-based salts) in the reduction process of lead chromate-based pigments, will be presented in the next section, by discussing the Cr-speciation results obtained from photochemically aged varnished paint models.

Aged Varnished Oil Paint Models: Cr-Speciation Measurements. After UVA-visible light exposure, the varnished S_{3D} ($PbCr_{0.2}S_{0.8}O_4$) samples clearly showed the formation of a brown layer on the outer surface, whereas only a minor chromatic alteration was observed for the S_{1mono} ($PbCrO_4$) paints (Figure 7A).

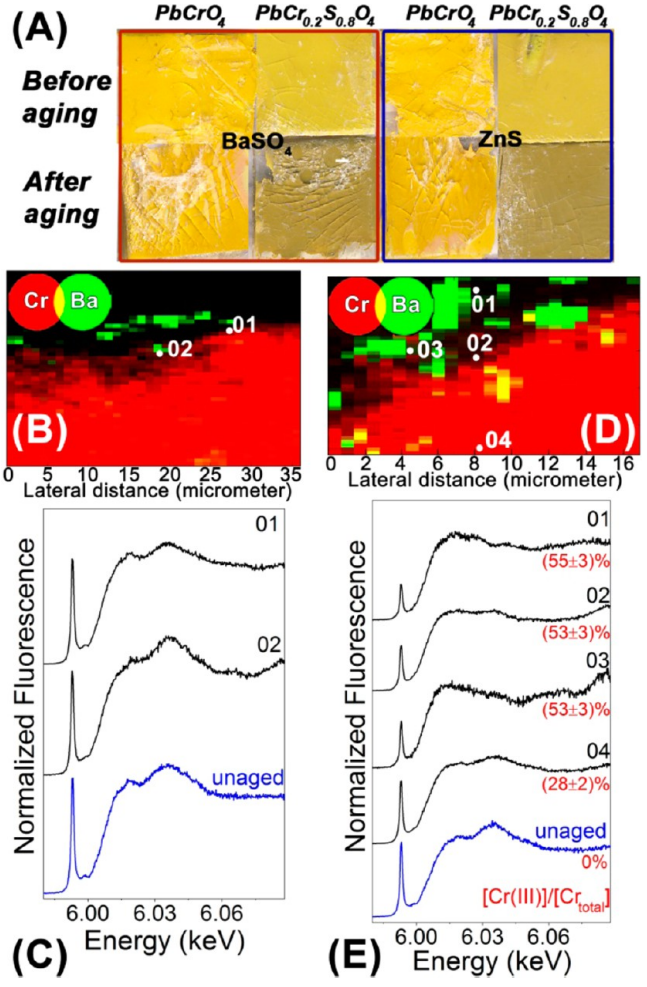

Figure 7. (A) Photographs of $PbCrO_4$ (S_{1mono}) and $PbCr_{0.2}S_{0.8}O_4$ (S_{3D}) model paints varnished with a dammar resin layer contaminated with either $BaSO_4$ ($S_{1mono\text{-}SO_4}{}^{2-}$, $S_{3D\text{-}SO_4}{}^{2-}$) or ZnS ($S_{1mono\text{-}S^{2-}}$, $S_{3D\text{-}S^{2-}}$) (top) before and (bottom) after photochemical aging. (B,D) RG composite images of Cr/Ba and (C,E) corresponding Cr K-edge XANES spectra of (B−C) $S_{1mono\text{-}SO_4}{}^{2-}$ and (D-E) $S_{3D\text{-}SO_4}{}^{2-}$ paints (pixel size: $1 \times 0.5\ \mu m^2$; dwell time: 100 ms). In (B, D), white labels indicate the regions where the profiles of (C, E) were acquired. In (E), red labels show the percentage relative amount of Cr(III).

Similar color changes were visible for the samples covered by a varnish layer containing either $BaSO_4$ ($S_{1mono\text{-}SO_4}{}^{2-}$, $S_{3D\text{-}SO_4}{}^{2-}$) or ZnS ($S_{1mono\text{-}S^{2-}}$, $S_{3D\text{-}S^{2-}}$). The behavior of these aged varnished paints appears to be comparable to that previously observed on the equivalent version of the unvarnished samples.[4]

dx.doi.org/10.1021/ac502841g | Anal. Chem. 2014, 86, 10804−10811

This qualitative information was confirmed by Cr K-edge XANES point measurements (Figure 7C,E) that were performed in the locations indicated by the XRF maps of Figure 7B,D. As examples, only the results obtained from samples $S_{1mono\text{-}SO_4}^{2-}$ and $S_{3D\text{-}SO_4}^{2-}$ are reported in Figure 7, because those acquired from $S_{1mono\text{-}S}^{2-}$ and $S_{3D\text{-}S}^{2}$ were very similar.

For $S_{1mono\text{-}SO_4}^{2-}$, μ-XANES spectra recorded either from the yellow paint/varnish interface or around the $BaSO_4$ particles inside the coating revealed profiles similar to those obtained from the corresponding unaged model sample (Figure 7C).

Regarding $S_{3D\text{-}SO_4}^{2-}$, XANES measurements (Figure 7E) showed a Cr speciation distribution similar to the equivalently aged unvarnished paint, the latter already described in Part 4.[4] The fraction of Cr(III) is around 55% at the interface (spectra 01−03), while it reaches a value of about 30% in the yellow paint below (ca. 8−9 μm in depth; spectrum 04). No differences were observed in the XANES profiles acquired from the Cr-rich areas around the $BaSO_4$ particles inside the varnish and those recorded at the interface (Figure 7E, cf. spectra 02 and 03).

In keeping with the results described in Part 4,[4] the profiles recorded at the interface and in the Cr-rich areas inside the varnish of sample $S_{3D\text{-}SO_4}^{2-}$ (spectra 01−03) were adequately described when the XANES spectra of $PbCr_{0.2}S_{0.8}O_4$, $Cr(OH)_3$, and either Cr(III)-sulfates [e.g., $KCr(SO_4)_2{\cdot}12H_2O$ or $Cr_2(SO_4){\cdot}H_2O$] or Cr(III)-organo metal compounds [such as Cr(III)-acetylacetonate or −acetate] were included in the fitting model (results not shown in detail). At greater depth, only two components [$PbCr_{0.2}S_{0.8}O_4$ and $Cr(OH)_3$/ Cr(III)-acetate] were necessary to fit the spectrum (profile 04).

Therefore, in summary, no detectable contribution to the degradation of lead chromate-based yellows from the resin and sulfide and sulfate salts have been observed. Relevant observation is that the dammar resin, despite absorbing the light in 200−300 nm wavelength range,[26,33] did not show a protective effect on the paint layer underneath. In fact, our previous studies,[3,4] proved the S-rich orthorhombic chrome-yellow (S_{3D}) is photosensitive not only when exposed to the UVA light but also at wavelengths higher than 300 nm.

CONCLUSIONS

As a continuation of our series of papers about the degradation process of chrome yellow pigments, in this work, synchrotron radiation-based μ-XRF and μ-XANES investigations were performed to gain new insights into the nature and distribution of Cr and S species at the paint/coating interface of three microsamples taken from originally uncoated artworks by Van Gogh and Gauguin (late 19th century), belonging to three different European museums.

In all the samples investigated, a degradation of the original $PbCr_{1-x}S_xO_4$ chrome yellow was found, as clearly demonstrated by the presence of Cr(III)-based compounds.

Regardless of the nature of the coatings (resins or wax), Cr and S K-edge μ-XRF and μ-XANES spectra revealed that the reduced Cr, often colocalized with sulfate species, was present not only at the paint/coating interface but also dispersed inside the varnish/wax layers in the form of micrograins. The Cr(III) distribution can be reasonably ascribed to the mechanical friction caused by applying the coating with a brush that picked up and redistributed loose Cr species, most probably already photoreduced at the surface of the original chrome yellow paint. Inside the coating and within the grain, the alteration compounds were present in abundance up to 70% and 100%, respectively, and were identified as Cr(III)-sulfates and Cr(III)-oxides. In one of the two Van Gogh's painting samples, indications of the presence of Cr(III)-organo metal compounds and Cr(III)-chlorides were also found. These results open up the possibility to use the analysis of removed coating material as a preliminary, minimally invasive tool for the assessment of the state of degradation of originally uncoated chrome yellow paint.

Due to the complex and heterogeneous composition of original micropaint samples, this study was not able to provide clear evidence for the fact that the coating and its constituents have influenced the chemical degradation of the paint. Nonetheless, insights were obtained by a preliminary study of photochemically aged chrome yellow paint models coated with a varnish layer contaminated with sulfide and sulfate salts. Within the boundaries of the current experimental conditions, we observed that the varnish did not act to protect against the photoreduction of chrome yellow paints. Neither could we detect any contribution of the S species present within the coating toward the degradation of this class of compounds.

Additional investigations are ongoing in order to (i) evaluate the effects of the coating application over aged chrome yellow paints on the Cr(III) compounds morphology and distribution; (ii) assess if and how other factors (e.g., relative humidity conditions higher than 40%) can play a significant role in activating the alteration pathways of chrome yellows.

ASSOCIATED CONTENT

Supporting Information

Additional information as noted in text. This material is available free of charge via the Internet at http://pubs.acs.org.

AUTHOR INFORMATION

Corresponding Author

*E-mail: letizia.monico@uantwerpen.be.

Notes

The authors declare no competing financial interest.

ACKNOWLEDGMENTS

This research was supported by the Italian projects PRIN (SICH) and PON (ITACHA). The text also presents results from Interuniversity Attraction Poles Programme−Belgian Science Policy (S2-ART project S4DA), GOA "XANES meets ELNES" (Research Fund University of Antwerp, Belgium) and FWO (Brussels, Belgium) projects no. G.0704.08 and G.01769.09. ESRF is acknowledged for the grants received (experiments EC-799 and EC-1051). L.M. acknowledges the CNR for the financial support received in the framework of the Short Term Mobility Programme 2013. Thanks are expressed to Ella Hendriks (Van Gogh Museum, Amsterdam) and Muriel Geldof (Cultural Heritage Agency of The Netherlands) for selecting and sharing the information on the cross-section taken from *Bank of the Seine*. All the staff of the Van Gogh Museum, the Kröller-Müller Museum, and the Musée d'Orsay are acknowledged for the agreeable cooperation.

REFERENCES

(1) Hendriks, E.; van Tilborgh, L. Vincent Van Gogh Paintings - Volume 2: Antwerp and Paris 1885-1888; Waanders Publishers: Zwolle and Van Gogh Museum: Amsterdam, 2011; pp 90−143.

(2) Vellekoop, M.; Geldof, M.; Hendriks, E.; Jansen, L.; de Tagle, A. *Van Gogh's Studio Practice*; Yale University Press: New Haven and London, 2013.

(3) Monico, L.; Van der Snickt, G.; Janssens, K.; De Nolf, W.; Miliani, C.; Verbeeck, J.; Tian, H.; Tan, H.; Dik, J.; Radepont, M.; Cotte, M. *Anal. Chem.* **2011**, *83*, 1214−1223.
(4) Monico, L.; Janssens, K.; Miliani, C.; Van der Snickt, G.; Brunetti, B. G.; Cestelli Guidi, M.; Radepont, M.; Cotte, M. *Anal. Chem.* **2013**, *85*, 860−867.
(5) Tan, H.; Tian, H.; Verbeeck, J.; Monico, L.; Janssens, K.; Van Tendeloo, G. *Angew. Chem., Int. Ed.* **2013**, *52*, 11360−11363.
(6) Monico, L.; Janssens, K.; Miliani, C.; Brunetti, B. G.; Vagnini, M.; Vanmeert, F.; Falkenberg, G.; Abakumov, A.; Lu, Y.; Tian, H.; Verbeeck, J.; Radepont, M.; Cotte, M.; Hendriks, E.; Geldof, M.; van der Loeff, L.; Salvant, J.; Menu, M. *Anal. Chem.* **2013**, *85*, 851−859.
(7) Burnstock, A. R.; Jones, C. G.; Cressey, G. *Kunsttechnol. Konserv.* **2003**, *17*, 74−84.
(8) Monico, L.; Janssens, K.; Hendriks, E.; Brunetti, B. G.; Miliani, C. *J. Raman Spectrosc.* **2014**, DOI: 10.1002/jrs.4548.
(9) Monico, L.; Van der Snickt, G.; Janssens, K.; De Nolf, W.; Miliani, C.; Dik, J.; Radepont, M.; Hendriks, E.; Geldof, M.; Cotte, M. *Anal. Chem.* **2011**, *83*, 1224−1231.
(10) Van der Snickt, G.; Janssens, K.; Dik, J.; De Nolf, W.; Vanmeert, F.; Jaroszewicz, J.; Cotte, M.; Falkenberg, G.; Van der Loeff, L. *Anal. Chem.* **2012**, *84*, 10221−10228.
(11) van der Weerd, J.; Geldof, M.; van der Loeff, L.; Heeren, R. M. A.; Boon, J. J. *Kunsttechnol. Konserv.* **2003**, *17*, 407−416.
(12) Kim, C.; Zhou, Q.; Deng, B.; Thornton, E. C.; Xu, H. *Environ. Sci. Technol.* **2001**, *35*, 2219−2225.
(13) Beukes, J. P.; Pienaar, J. J.; Lachmann, G.; Giesekke, E. W. *Water S A* **1999**, *25*, 363−370.
(14) Plummer, L. N. *Econ. Geol.* **1971**, *66*, 252−258.
(15) Machel, H. G. *Sediment. Geol.* **2001**, *140*, 143−175.
(16) Salomé, M.; Cotte, M.; Baker, R.; Barrett, R.; Benseny-Cases, N.; Berruyer, G.; Bugnazet, D.; Castillo-Michel, H.; Cornu, C.; Fayard, B.; Gagliardini, E.; Hino, R.; Morse, J.; Papillon, E.; Pouyet, E.; Rivard, C.; Solé, V. A.; Susini, J.; Veronesi, G. *J. Phys.: Conf. Ser.* **2013**, *425*, 182004.
(17) Rosi, F.; Miliani, C.; Clementi, C.; Kahrim, K.; Presciutti, F.; Vagnini, M.; Manuali, V.; Daveri, A.; Cartechini, L.; Brunetti, B. G.; Sgamellotti, A. *Appl. Phys. A: Mater. Sci. Process.* **2010**, *100*, 613−624.
(18) Lazzari, M.; Chiantore, O. *Polym. Degrad. Stab.* **1999**, *65*, 303−313.
(19) Burgio, L.; Clark, R. J. *Spectrochim. Acta, Part A* **2001**, *57*, 1491−1521.
(20) Miliani, C.; Rosi, F.; Daveri, A.; Brunetti, B. G. *Appl. Phys. A: Mater. Sci. Process.* **2012**, *106*, 295−307.
(21) Nakamoto, K. *Infrared and Raman spectra of inorganic and coordination compounds*, 4th ed; John Wiley & Sons Inc.: New York, 1986.
(22) Eastaugh, N.; Walsh, V.; Chaplin, T.; Siddall, R. *The Pigment Compendium: a dictionary of historical pigments*; Elsevier Butterworth-Heinemann: Amsterdam and Boston, 2004.
(23) Gysels, K.; Delalieux, F.; Deutsch, F.; Van Grieken, R.; Camuffo, D.; Bernardi, A.; Sturaro, G.; Busse, H. J.; Wieser, M. *J. Cult. Herit.* **2004**, *5*, 221−230.
(24) De Bock, L. A.; Van Grieken, R.; Camuffo, D.; Grime, G. W. *Environ. Sci. Technol.* **1996**, *30*, 3341−3350.
(25) Saunders, D. *National Gallery Technical Bulletin* **2000**, *21*, 77−94.
(26) Feller, R. L.; Stolow, N.; Jones, E. H. *On Picture Varnishes and Their Solvents*; National Gallery of Art: Washington DC, 1985.
(27) Pantelouris, A.; Modrow, H.; Pantelouris, M.; Hormes, J.; Reinen, D. *Chem. Phys.* **2004**, *300*, 13−22.
(28) Cotte, M.; Susini, J.; Metrich, N.; Moscato, A.; Gratziu, C.; Bertagnini, A.; Pagano, M. *Anal. Chem.* **2006**, *78*, 7484−7492.
(29) Vairavamurthy, A. *Spectrochim. Acta, Part A* **1998**, *54*, 2009−2017.
(30) Ernst, G.; Rolf, P.; Hans-Dieter, S. U.S. Patent 3,448,079, 1969.
(31) Girard, T. A. U.S. Patent 3,223,536, 1965.
(32) Zanella, L.; Casadio, F.; Gray, K. A.; Warta, R.; Ma, Q.; Gaillard, J. F. *J. Anal. Atom. Spectrom.* **2011**, *26*, 1090−1097.
(33) de la Rie, E. R. *Anal. Chem.* **1989**, *61*, 1228A−1240A.